

Ion Exchange Treatment of Groundwater Contaminated by Arsenic in the Presence of Sulphate. Breakthrough Experiments and Modeling

Agostina Chiavola · Emilio D'Amato · Renato Baciocchi

Received: 9 August 2011 / Accepted: 24 November 2011 / Published online: 20 December 2011
© Springer Science+Business Media B.V. 2011

Abstract This report deals with the application of ion exchange columns to the treatment of groundwater contaminated by high concentrations of arsenic in the presence of sulphates. Two different process layouts were tested, based on the use of a single column and of two-in-series columns, respectively. Several breakthrough tests were performed, where the effect of the operating parameters, as the influent flow rate, the packed bed height and the feed water composition, were investigated. The collected data were described using three different modeling approaches, based on the Bohart–Adams, Yan and Thomas models, respectively. These models were all found to describe the experimental data with a quite good agreement (based

on the R^2 value). The ion exchange capacity evaluated by the models (about 3.8 mEq/g) was comparable with the value provided by the supplier (3.8 mEq/g), but higher than the value determined through batch tests of a previous study by the same authors. The models were then successfully applied to describe the breakthrough behaviour of the two in-series column plant using a real feed contaminated by high arsenic concentrations in the presence of sulphate.

Keywords Arsenic · Breakthrough · Column plant · Exhaustion · Ion exchange resin · Sulphates

Abbreviations

As	Arsenic
As(V)	Pentavalent arsenic
As(III)	Trivalent arsenic
MAC	Maximum admissible concentration
IE	Ion exchange
BKT	Breakthrough
EX	Exhaustion
t	Time (h)
C_t	Effluent concentration (mg/l or $\mu\text{g/l}$)
C_0	Influent concentration (mg/l or $\mu\text{g/l}$)
V_b	Bed volume (ml)
W_b	Weight of bed resin (mg)
Q	Influent flow rate (ml/min)
EBCT	Empty bed contact time (min)
q_{IE}	Resin uptake capacity (mg)
q_{IN}	Total amount of arsenic fed to the column at time t (mg)

A. Chiavola (✉)
Faculty of Engineering, Dipartimento di Ingegneria Civile,
Edile e Ambientale, Sapienza University of Rome,
Via Eudossiana, 18,
00184 Rome, Italy
e-mail: agostina.chiavola@uniroma1.it

E. D'Amato
Faculty of Engineering,
Dipartimento di Ingegneria Civile e Ambientale,
University of Florence,
Via S. Marta 3,
50139 Florence, Italy

R. Baciocchi
Faculty of Engineering, Dipartimento di Ingegneria Civile,
University of Rome Tor Vergata,
Via del Politecnico, 1,
00133 Rome, Italy

$R\%$	Total ion removal (%)
T	Temperature ($^{\circ}\text{C}$)
F1 and F2	Real feed waters
BDST	Bed depth-service-time
k_{BA}	Bohart–Adams rate constant (l/h mg)
Z	Bed depth (m)
N_0	Maximum solid phase capacity per unit volume of bed (mg/l)
μ	Superficial liquid velocity (m/h)
A	Cross section surface of the resin bed (m^2)
q_{BA}	Maximum solid phase capacity per unit weight of bed estimated by the Bohart–Adams model (mg/g)
k_{T}	Thomas rate constant (l/h mg)
q_{T}	Maximum solid phase capacity per unit weight of bed estimated by the Thomas model (mg/g)
V	Throughput volume (l)
a_{mdr}	Modified dose–response model constant (unit-less)
t_{BKT}	BKT time (min)
t_{EX}	EX time (min)
$E_{\text{R}}\%$	Efficiency of the regeneration phase (%)
$\text{SO}_4(\text{theo})$	Expected sulphates in the spent brine solution (mg/l)
$\text{SO}_4(\text{exp})$	Measured sulphates in the spent brine solution (mg/l)

1 Introduction

Arsenic (As) is a widespread element, found in the atmosphere, soils and rocks, natural water and living organisms. Although it is produced by several anthropogenic activities, most of the environmental issues are related to the presence of arsenic due to natural processes, such as weathering reactions, biological activity and volcanic emissions, which affect the concentration of arsenic in various environmental matrices, including specifically groundwater resources (Smedley and Kinniburgh 2002). The increasing concern posed by high As concentration in several aquifers used as drinking water source, has prompted the European Community (EU), including Italy, to reduce the maximum admissible concentration (MAC) of arsenic in drinking water to 10 $\mu\text{g/l}$ from the previous 50 $\mu\text{g/l}$ level (European Directive 98/83 and Italian Legislative decree 31/2001). The need to reduce As

concentration to comply with the new regulatory limits has urged local authorities and companies managing the integrated water systems to evaluate the most appropriate solutions to address this issue. Among the different options, such as the replacement of the contaminated water source, or mixing it with a non-contaminated one, groundwater treatment needs also to be considered and will be discussed in this paper.

Arsenic can be found in the -3 , 0 , $+3$ and $+5$ oxidation states. Its environmental forms include arsenious acids, arsenic acids, arsenites, arsenates, methylarsenic acid, dimethylarsinic acid and arsine. Arsenite (AsO_3^{3-}) and arsenate (AsO_4^{3-}), referred to as arsenic(III) and arsenic(V), respectively, are the most common forms in groundwater and surface water. As(V) prevails in oxygen rich aerobic environments, whereas As(III) is more common in moderately reducing anaerobic environments typically found in groundwater. In the pH range of natural water, As(V) is found in ionized forms as H_2AsO_4^- and HAsO_4^{2-} , whereas As(III) is in the undissociated form (Frankenberger 2001; Jain and Ali 2000). Arsenic can be removed from water through several physicochemical processes, including coagulation with iron and aluminum salts, adsorption on different iron-based materials, and ion exchange resin (IER) processes (Ming-Cheng 2005; US EPA 2000, 2003; Viraraghavan et al. 1999). All these processes preferentially target As(V), thus requiring a preliminary treatment aimed at oxidizing As(III) to As(V) (Clifford and Ghurye 2001).

Ion exchange processes have been shown to be suitable to treat As-contaminated drinking water when this element is in the ionized form (Helferrich 1962; Korngold et al. 2001; Mohan and Pittman 2007). The main advantages with respect to other alternative treatments are: high removal efficiency, low chemical requirements, no modification of drinking water organoleptic properties. However, the affinity of the IER for arsenic can be affected by the presence of other anions (e.g., sulphates) in water which may compete with arsenic for the ion exchange active sites. When these competitive anions are present at high concentrations, the As removal capacity can be significantly reduced and consequently the frequency of resin regeneration increased as well as the treatment costs. Different alternative schemes and operating strategies of ion exchange treatment units have been therefore proposed to overcome such limitations. For instance,

Kim et al. (2003) proposed a novel approach for operating the ion exchange process for the treatment of As-rich effluents in the presence of sulphates. In conventional ion exchange practice, the resin would be regenerated significantly before As(V) breakthrough occurred to provide a safety factor to protect against As entry into the distribution system. In the modified treatment process tested by Kim et al. (2003), two ion exchange columns are operated in series, and the upstream column is regenerated after the As(V)-rich zone has passed completely out of the column but long before As appears in the effluent from the downstream column. The regenerated column is then returned to the system in the downstream position, and the process is repeated. Using this layout, arsenic is accumulated in the system, cycle after cycle. The regeneration step is performed on a column saturated almost exclusively with sulphates, whereas producing a regenerant brine that is virtually As-free. Therefore, brine can be recycled after sulphate removal by precipitation as barium or calcium salt. Kim et al. (2003) have demonstrated the feasibility of this process for the treatment of water containing 40 µg/l As (V) and 80 mg/l sulphates. Kim and Benjamin (2004) have then applied this process to water containing up to 40 µg/l As(V), together with sulphates from 80 to 125 mg/l and nitrates from 30 to 60 mg/l, and also proposed a short-cut modeling of the process.

Despite some information on the breakthrough behaviour of the As/SO₄²⁻ system on IER that was provided in the papers cited above, it is worth noting that few data on the application of this plant to higher arsenic and sulphate concentrations, are available in the literature. Moreover, most of the references report on experiments performed with model solutions without a further validation under actual operating conditions. These data could provide a sound reference for a proper process development and design in the case of highly contaminated groundwater. Modeling of the ion exchange process can also help in predicting the performance of the ion exchange process (Benefield et al. 1982; Treybal 1981). This can also support us in evaluating the technical–economical feasibility of the ion exchange process as compared to the alternative treatment systems.

This paper focuses on the treatment of groundwater contaminated by arsenic in the presence of sulphates through the ion exchange process. The authors have previously studied and modeled ion exchange

equilibria of As(V) on strong anionic resin, in the presence of nitrates and sulphates (Baciocchi et al. 2005). However, data collected from batch systems cannot be directly applied to continuous processes, which are usually performed in columns in full-scale applications. Therefore, continuous ion exchange (IE) studies are needed to describe the column process and to scale it up for practical applications.

The present study reports the results of an experimental study carried out on column loaded with an IER. Two different schemes were tested: (1) one single column and (2) two-in-series columns. Several experimental tests were carried out in both laboratory-scale plants, evaluating the effects of modifying the operating conditions. The obtained breakthrough curves were then modeled and the values of the main constants of the best fitting model determined. The results of the modeling activity were then compared with the results of column tests performed with a real influent feed, obtained by spiking tap water at different arsenic and sulphates concentrations.

2 Methods

2.1 Resin

The resin used in this work was Amberlite® IRA400 Cl, provided by Rohm and Haas. This is a type I, gel-like premium grade, strongly basic, anion exchange resin, based on a cross-linked polystyrene, which exchanges chlorides. The main properties are shown in Table 1. The resin was used as received, without any conditioning step.

2.2 Column Plant Layout

Breakthrough experiments were performed on clean and dry glass columns of 15 cm length and 1.3 cm internal diameter, packed with various weights of IER (W_b) as detailed in Table 2.

The columns were continuously fed in a down-flow mode using a peristaltic pump. Two different schemes of the IE plant were tested: (1) one single column and (2) two-in-series columns as proposed by Kim et al. (2003). Effluent samples were collected at different time intervals and then analyzed to monitor the contaminant concentration leaving the column. The breakthrough and exhaustion conditions (BKT and EX,

Table 1 Main properties of the resin

Parameter	
Matrix	Polystyrene divinylbenzene copolymer
Functional groups	Quaternary ammonium
Ionic form	Chloride
Total exchange capacity	$\geq 3.8 \text{ mEq g}^{-1}$ (Cl ⁻ form)
Moisture holding capacity	40–47% (Cl ⁻ form)
Harmonic mean size	0.60–0.75 mm
Uniformity coefficient	≤ 1.6

respectively) were considered achieved when the effluent concentration (C_t) was equal to 5% and 95% of the influent concentration (C_0), respectively. The breakthrough curves were drawn by plotting C_t/C_0

versus the throughput volumes measured in terms of multiple-valued of bed volumes (V_b).

2.3 Regeneration

The resin in the column after sulphate EX was regenerated using 300 ml of a 3 M NaCl solution, followed by washing with 50 ml ultrapure water. A fresh regeneration solution was always used.

2.4 Feed Solutions

Various feed solutions were used for the tests. The model solutions (referred to as Model) were prepared by dissolving in ultrapure water known amounts of $\text{AsHNa}_2\text{O}_4 \cdot 7\text{H}_2\text{O}$ so as to achieve the desired As(V)

Table 2 List of the experimental conditions

BKT tests	SO_4^{-2} (mg l ⁻¹)	As ($\mu\text{g l}^{-1}$)	Q (ml min ⁻¹)	W_b (g)	V_b (ml)	EBCT (min)	Influent solution
1	100	0	6.0	4.8	10.6	1.8	Model
2	200	0	6.0	4.8	10.6	1.8	Model
3	100	100	6.0	4.8	10.6	1.8	Model
4	200	100	6.0	4.8	10.6	1.8	Model
5	100	0	3.8	4.8	10.6	2.8	Model
6	100	0	4.8	4.8	10.6	2.2	Model
7	100	0	7.0	4.8	10.6	1.5	Model
8	200	0	3.8	4.8	10.6	2.8	Model
9	200	0	4.8	4.8	10.6	2.2	Model
10	200	0	7.0	4.8	10.6	1.5	Model
11	100	100	4.8	4.8	10.6	2.2	Model
12	200	100	4.8	4.8	10.6	2.2	Model
13	100	0	6.0	3.0	6.6	1.1	Model
14	100	0	6.0	3.8	8.4	1.4	Model
15	100	0	6.0	4.8	10.6	1.8	Model
16	100	0	6.0	6.0	13.2	2.2	Model
17	100	0	6.0	7.0	15.4	2.6	Model
18	200	0	6.0	3.0	6.6	1.1	Model
19	200	0	6.0	3.8	8.4	1.4	Model
20	200	0	6.0	4.8	10.6	1.8	Model
21	200	0	6.0	6.0	13.2	2.2	Model
22	200	0	6.0	7.0	15.4	2.6	Model
23	100	100	6.0	4.8	10.6	1.8	Model
24	200	100	6.0	4.8	10.6	1.8	Model
25	17.9	100	6.0	4.8	10.6	1.8	F1
26	100	100	6.0	7.0	15.4	2.6	F2

concentrations. Similarly, different weights of Na_2SO_4 were dissolved in ultrapure water to determine the prefixed sulphate concentrations in the feeding solutions. Real feed solutions (referred to as F1 and F2) were obtained by spiking tap water (average composition: 17.9 mg $\text{SO}_4^{2-}/\text{l}$, 5.9 mg Cl^-/l , 3.4 mg NO_3^-/l , 279.4 mg HCO_3^-/l) with arsenic (As(V)) only and arsenic and sulphates, respectively, following the same procedure described above. The different feeding solution compositions are listed in Table 2.

The arsenic-containing solutions were always spiked with 100 μl H_2O_2 (30% v/v) in order to maintain a positive oxidation–reduction (Redox) potential during the whole duration of the experiment, so as to keep arsenic in its original pentavalent oxidation state, as also outlined by Baciocchi et al. (2005).

2.5 Experimental Conditions

Table 2 reports the operating conditions of the performed tests, with V_b , W_b , Q and EBCT standing for bed volume and bed weight of the resin packed within each column, influent flow rate and empty bed contact time (EBCT), respectively. The EBCTs were calculated as follows:

$$\text{EBCT} = \frac{V_b}{Q} \quad (1)$$

Temperature of the tests was always maintained at $T=20\pm 2^\circ\text{C}$.

2.6 Analytical Methods

Arsenic was analyzed using a Model 3030B Atomic Absorption Spectrophotometer equipped with a graphite furnace (Perkin-Elmer, USA) using the hydride method (APHA/AWWA/WEF 1998).

Sulphates were analyzed by a Model 761-IC Ion Chromatography system (Metrohm), using a DualOne column (Metrohm).

Results obtained were found to be reproducible within $\pm 3\%$.

2.7 Calculation of the Ion Exchange Column Efficiency

The ion mass removed by the resin at time t (uptake capacity, q_{IE}) was calculated from the area above the

breakthrough curve (outlet ion concentration versus time), as shown below:

$$q_{\text{IE}} = C_0 Q \int_a^t \left(1 - \frac{C_t}{C_0}\right) dt \quad (2)$$

where C_0 is the influent concentration (mg/l), C_t is the effluent concentration at time t (mg/l), and Q is the volumetric influent flow rate (l/h). The integral term of Eq. 2 was solved numerically. The total amount of arsenic fed to the column at time t , q_{IN} , was calculated as follows:

$$q_{\text{IN}} = C_0 Q t \quad (3)$$

Therefore, the total ion removal ($R\%$) was determined through Eq. 4:

$$R\% = \frac{q_{\text{IE}}}{q_{\text{IN}}} \times 100 \quad (4)$$

3 Mathematical Modeling

The mathematical modeling has a key role in the scale-up procedure from laboratory experiments through pilot plant to industrial scale. It can help to analyze and to explain experimental data, to identify mechanisms relevant to the process, to predict changes due to different operating conditions, and to optimize the overall efficiency of the process (Borba et al. 2008).

The features of the different mathematical models used to describe the results of the breakthrough experiments are discussed in the following sections.

3.1 Bohart–Adams Model

The first model, known as the bed depth–service–time model (BDST), is based on the Bohart–Adams theory (Bohart and Adams 1920). This model relies on the assumption of rectangle or step isotherm, with the capacity of the adsorbent set to a constant value, and on considering the rate of IE proportional to the interstitial concentration of the adsorbate in the liquid phase and the unused capacity of the solid. As a result, it provides the following solution to the mass balance equation through the column:

$$\ln\left(\frac{C_0}{C_t} - 1\right) = k_{\text{BA}} N_0 \frac{Z}{\mu} - k_{\text{BA}} C_0 t \quad (5)$$

where C_t is the effluent concentration at time t (mg/l), C_0 is the influent concentration (mg/l), k_{BA} is the Bohart–Adams rate constant (l/h mg), Z is the bed depth (m), N_0 is the maximum solid phase capacity per unit volume of bed (mg/l), μ is the superficial liquid velocity (m/h) and t is the flow time (h).

The BDST model provides a linear relationship between the time required to reach the desired effluent concentration and the bed depth (Z), that is,

$$t = \frac{N_0}{C_0\mu}Z - \frac{1}{C_0k_{BA}} \ln\left(\frac{C_0}{C_t} - 1\right) \quad (6)$$

By replacing μ with Q/A , where A is the cross section surface of the bed, and considering the resin bed volume $V_b=ZA$, Eq. 6 can be rewritten as:

$$t = \frac{N_0V_b}{C_0Q} - \frac{1}{C_0k_{BA}} \ln\left(\frac{C_0}{C_t} - 1\right) \quad (7)$$

The values of k_{BA} and N_0 can be determined from the experimental data of the breakthrough curves by plotting t versus V_b . Once N_0 is known, then it is possible to calculate the value of q_{BA} , the maximum solid phase capacity per unit weight of bed (mg/g).

3.2 Thomas Model

The Thomas model is one of the most general and widely used models to describe column performance. It has been originally derived from the Bohart and Adams analysis. The expression by Thomas for an adsorption or IE column is given as follows (Thomas 1944):

$$\frac{C_t}{C_0} = \frac{1}{1 + \exp\left(\frac{k_T q_T W_b}{Q} - k_T C_0 t\right)} \quad (8)$$

where C_t , C_0 , t , W_b and Q were previously defined; k_T is the Thomas rate constant (l/h mg) and q_T is the maximum solid phase concentration estimated by the Thomas model (mg/g).

The linearized form of the Thomas model is as follows:

$$\ln\left(\frac{C_0}{C_t} - 1\right) = \frac{k_T q_T W_b}{Q} - k_T C_0 t \quad (9)$$

The values of k_T and q_T can be determined from the experimental data by plotting $\ln(C_0/C_t - 1)$ versus t at a given flow rate.

3.3 Yan Model

Yan et al. (2001) proposed a modified dose–response model, which minimizes the error that results from the use of the Thomas model, especially at very small and very large operation times. The Yan model can be formulated as follows (Senthilkumar et al. 2010):

$$\frac{C_t}{C_0} = 1 - \frac{1}{1 + \left(\frac{VC_0}{q_Y W_b}\right)^{a_{\text{mdr}}}} \quad (10)$$

where V represents the throughput volume (l), a_{mdr} is the modified dose–response model constant (unitless), whereas the other parameters are as defined above.

The linearized form of Eq. (10) is shown below:

$$\ln\left(\frac{C_0}{C_t} - 1\right) = a_{\text{mdr}} \ln\left(\frac{W_b q_Y}{C_0}\right) - a_{\text{mdr}} \ln(V) \quad (11)$$

Same as above, the values of a_{mdr} and q_Y can be determined from the experimental data by plotting $\ln((C_0 - C_t)/C_t)$ versus $\ln V$.

4 Results and Discussion

4.1 Effect of Feed Concentration (BKT Tests 1–4)

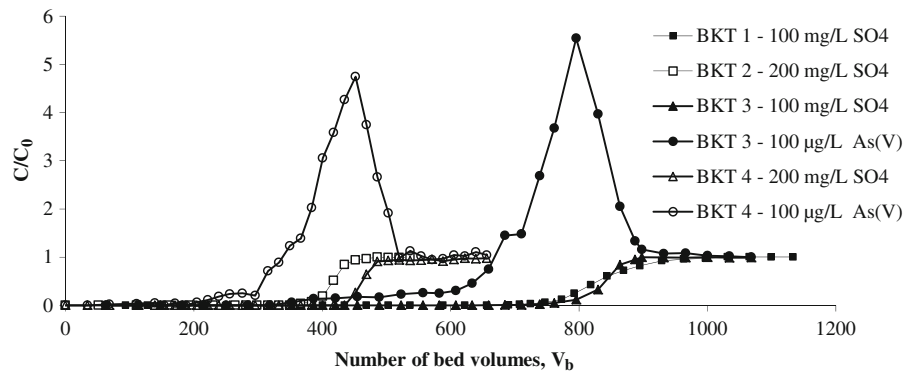
The single column scheme of the IE plant as described in Section 2.2 was applied in this set of tests. Model solutions containing arsenic and/or sulphates were continuously fed to the plant until EX conditions were achieved.

Figure 1 shows the breakthrough curves of arsenic and sulphates obtained for various feed water compositions, where V_b on the x -axis refers to the number of bed volumes.

Breakthrough and exhaustion conditions were attained more rapidly as the feed water contaminant load increased; moreover, the shape of the curves became steeper for higher feed concentrations.

It is worth noting that As(V) breakthrough took place in a relatively short time, that is, after 200 V_b and 330 V_b for 200 and 100 mg/l sulphate feed concentrations, respectively. As expected, a pulse enriched in As(V) developed in the column, whereas sulphates eluted after 440 V_b and 760 V_b , respectively. This pattern was a consequence of the lower affinity of As(V) for the active exchange sites of the resin with

Fig. 1 Breakthrough curves at different feed compositions



respect to sulphates. As reported by several groups (Clifford 1999; Mudhoo et al. 2011), due to their higher selectivity, in an IE column, sulphates binds upstream of As(V); therefore, an As(V)-rich zone is progressively pushed downstream as SO_4 saturates the upstream binding sites and move into the As-rich zone. Ultimately, if the run continues until SO_4 arrives at the end of the column, As(V) is displaced into the effluent as a chromatographic peak with a concentration that can be much higher than its influent concentration (Ghurye et al. 1999).

Breakthrough experiments performed with solutions not containing As(V) provided a similar behaviour for sulphates, as shown in the same figure. Hence, the presence of arsenic in a significantly lower concentration did not notably affect the sulphate removal.

As the sulphate breakthrough was shown to control the column saturation, independently from As concentration, most of the following BKT experiments were performed in feeding sulphate only.

4.2 Effect of EBCT (BKT Tests 1–12)

The single-column scheme was also used in this set of tests, which were performed feeding a model solution. Figure 2 shows the eight BKT curves obtained varying the influent flow rates, Q , and using two different sulphate concentrations, equal to 100 and 200 mg/l, respectively. Two of these BKT curves were obtained by adding arsenic to the feed in order to verify its influence on sulphate breakthrough curves.

As expected, the BKT and the EX times increased with decreasing flow rates. A reasonably good linear correlation was found between both t_{BKT} and t_{EX} and the corresponding EBCTs, respectively.

Moreover, as the flow rate increased, sulphate concentration in the effluent increased more rapidly resulting in a much sharper breakthrough curve. The presence of arsenic did not notably affect the results.

The values of t_{BKT} and t_{EX} measured at the different EBCTs are listed in Table 3 for 100 and 200 mg/l SO_4^{2-} , respectively. In the same table, the total treated volume, the contaminant uptake and removal ($R\%$) are also shown. The percentage removal, $R\%$, was estimated from the mass balance performed at the exhaustion condition of the resin bed: since at this time arsenic was completely eluted from the column, the mass balance was calculated on sulphates only.

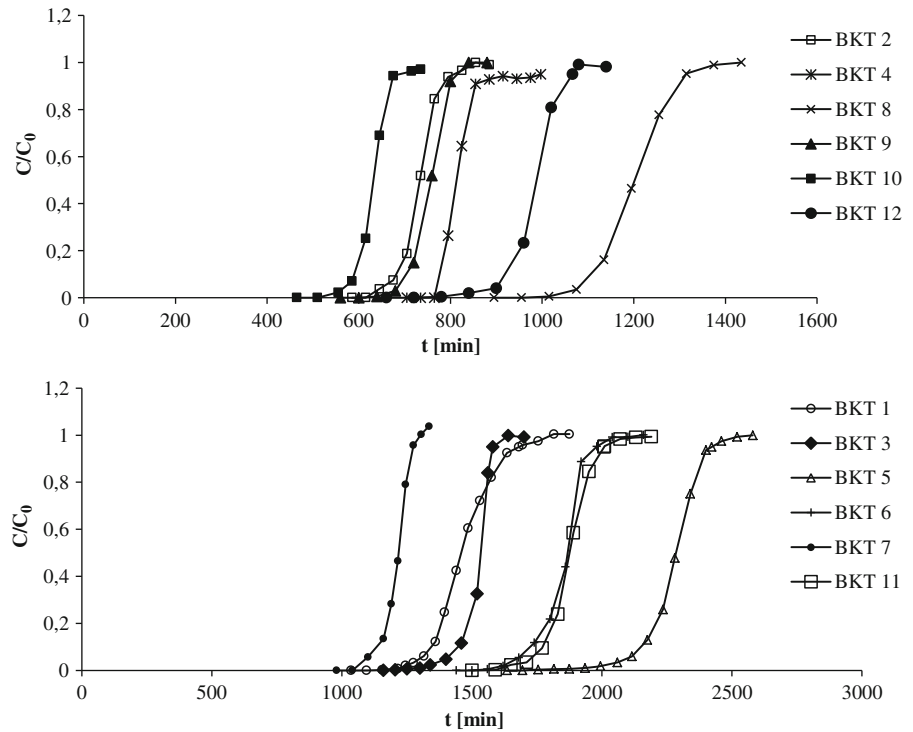
No significant difference was observed in the volume, uptake and removal values at increasing influent flow rates, that is, decreasing the EBCT. This might indicate that there was no limitation due to mass transfer in the liquid phase in the investigated operating range of flow rate. The values of the percentage removal and contaminant uptake were very high, 90% and 180 mg/g as average, respectively, without any significant change neither at higher sulphate concentration nor in the presence of arsenic.

Due to the more rapid achievement of resin saturation, the treated volume decreased significantly at increasing sulphate concentrations in the feed, with average values of 9.5 and 5.2 l at 100 and 200 mg/l SO_4^{2-} , respectively.

4.3 Effect of Bed Volume (BKT Tests 13–24)

IE removal in a packed column is largely dependent on the quantity of resin inside the column.

In this set of tests, performed with a single-column plant and model solutions, the influence of the height

Fig. 2 Breakthrough curves at different flow rates

of the bed resin, Z , and consequently of the bed volume, V_b , on the operation of the column plant was investigated. The different values of the bed heights were obtained by properly modifying the weight of the column packing resin, W_b .

Table 4 reports the values of t_{BKT} and t_{EX} as a function of the corresponding V_b , for the different feed water compositions. As expected, the breakthrough

and the exhaustion times were observed to decrease for lower column heights as a result of the reduced hydraulic residence time which limited the time for the contaminant mass transfer to occur from the liquid to the solid phase. Besides, the lower mass of resin determined a reduced availability of the active IE sites; consequently, the saturation condition was achieved more rapidly.

Table 3 Influence of the empty bed contact time

	EBCT (min)	t_{BKT} (min)	t_{EX} (min)	Volume (l)	Uptake (mg g^{-1})	$R\%$ (%)
100 mg/l SO_4^{2-}	1.5	1,093	1,274	8.9	172	95
	1.8	1,300	1,680	10.1	187	87
	2.2	1,673	1,980	9.5	179	93
	2.8	2,095	2,422	9.2	176	92
100 mg/l SO_4^{2-} +100 $\mu\text{g/l As(V)}$	1.8	1,342	1,562	9.4	182	94
	2.2	1,725	2,008	9.6	184	93
200 mg/l SO_4^{2-}	1.5	571	767	5.4	180	91
	1.8	657	808	4.8	178	91
	2.2	858	1,019	4.9	153	93
	2.8	1,083	1,314	5.0	189	91
200 mg/l SO_4^{2-} +100 $\mu\text{g/l As(V)}$	1.8	771	997	6.0	194	82
	2.2	903	1,067	5.1	178	88

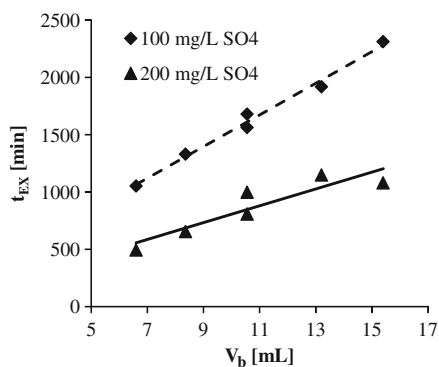
Table 4 Influence of the bed volume

	V_b (ml)	t_{BKT} (min)	t_{EX} (min)
100 mg/l SO_4^{2-}	15.4	2,014	2,311
	13.2	1,635	1,918
	10.6	1,300	1,680
	8.4	927	1,331
	6.6	783	1,053
100 mg/l SO_4^{2-} +100 $\mu\text{g/l}$ As(V)	10.6	1,342	1,562
200 mg/l SO_4^{2-}	15.4	886	1,079
	13.2	859	1,147
	10.6	657	807
	8.4	515	655
	6.6	365	494
200 mg/l SO_4^{2-} +100 $\mu\text{g/l}$ As(V)	10.6	770	997

4.4 Column Data Modeling

The breakthrough curves experimentally determined in BKT tests from 5 to 24 were described with the three different mathematical models presented in Section 3, and their agreement evaluated. The fitting was performed using the linear regression of the experimental results. Based on the value of R^2 , the best fitting model was identified. Then, the values of the maximum solid phase concentration on the IE resin and of the IE rate constant were calculated.

The linear plots resulted from the application of these models are shown in Figs. 3 and 4 for Bohart–Adams, Yan and Thomas models, respectively, referring to sulphate exhaustion conditions. In both figures, the results of model simulation of As(V) exhaustion are also shown. In Fig. 3, in particular, these values are

**Fig. 3** Bohart–Adams model representation

indicated by the double point at the EBCT value of 1.8 min.

The model parameters were determined from the intercept and the slope of these plots and the results obtained are displayed in Table 5 with the corresponding R^2 values.

A pretty good fitting between experimental data and model results was provided by all the applied models. Similar values of the fitting parameter k were obtained with Bohart–Adams and Thomas models, with 0.012 l/h mg as average, corresponding to 0.57 l/h mEq.

The three models also provided similar results for q — 182 mg/g (3.8 mEq/g) — at 100 mg/l, which also corresponded to the uptake value experimentally determined (Section 4.2). The models slightly overestimated the value of q at 200 mg/l SO_4^{2-} , particularly the Bohart–Adams model (4.0 vs. 3.7 mEq/g). Nonetheless, these values are in a good agreement with the theoretical value provided by the manufacturer, which is equal to 3.8 mEq/g. By contrast, they are slightly higher than the value obtained by the same authors in a previous work through batch trials (about 3.3 mEq/g) (Baciacchi et al. 2005). The difference between the IE capacity determined through column experiments and batch tests is reasonably due to the different experimental setup, as a higher capacity of the resin is expected in a column test where the surface is continuously exposed to fresh solution.

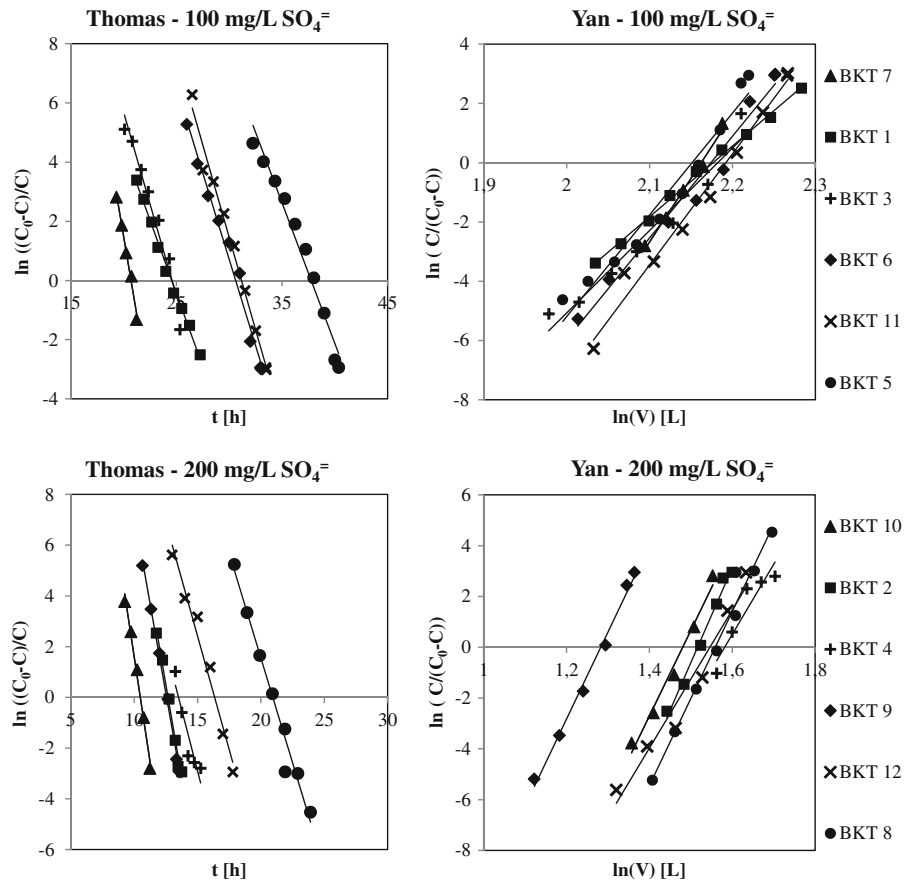
Since the linearization was performed by accounting for all the experimental data of the breakthrough curves up to the exhaustion time, it can be assessed that the three models tested seem to be suitable to predict both the BKT and EX times. Therefore, they can be used to determine also the time for which the MAC is achieved in the effluent, and consequently the service time of the column before regeneration is needed.

4.5 Two-in-Series Columns (BKT Tests 25–26)

This set of tests was performed with the aim of evaluating the feasibility of the previous modeling activity in the case of a real feed water highly contaminated in arsenic and sulphates. Furthermore, performances of the two-in-series column plant layout were evaluated, by investigating both the operation and regeneration stages.

In this scheme, the upstream column (column A) is continuously fed with an arsenic and sulphate-rich

Fig. 4 Thomas and Yan model representations



water. Due to the higher affinity of sulphates to the resin, arsenic is eluted first from column A and delivered to column B (downstream). When column A reaches sulphate exhaustion, arsenic has been already completely eluted from this column but it is too far from the outlet of the downstream column to appear in the effluent from the column. At this point, column A undergoes regeneration whereas column B is moved to the upstream position. The regenerated column is then

returned to the system in the downstream position and the process is then repeated.

In test 27, the system was fed with a solution (F1) spiked with 100 µg/l arsenic, whereas sulphates were at about 18 mg/l. The two in-series columns were operated for one cycle, until arsenic concentration in the effluent from column B have increased up to the MAC set by the EU legislation for drinking water ($C_t/C_0=0.1$).

Table 5 Average model parameters and R^2 values of Eqs. 7, 9 and 11

	Bohart–Adams			Yan			Thomas		
	R^2	k_{BA} ($l\ h^{-1}\ mg^{-1}$)	q_{BA} ($mg\ g^{-1}$)	R^2	$a_{m\text{dr}}$ (unit-less)	q_Y ($mg\ g^{-1}$)	R^2	k_T ($l\ h^{-1}\ mg^{-1}$)	q_T ($mg\ g^{-1}$)
100 mg/l SO_4^{2-}	0.97	0.011	182	0.98	33.5	181	0.97	0.013	182
100 mg/l SO_4^{2-} +100 µg/l As(V)									
200 mg/l SO_4^{2-}	0.83	0.012	194	0.96	31.4	187	0.97	0.012	187
200 mg/l SO_4^{2-} +100 µg/l As(V)									

By continuously feeding the plant, it was observed that chlorides were immediately released from column A at the beginning of the test since they were exchanged by the other anions present in the feed water, such as bicarbonates, which have higher affinity for the active sites of the resin. For instance, chloride concentration in the effluent from column A achieved the feed concentration after about 2,500 V_b treated, which corresponded approximately to the exhaustion time of bicarbonates. Nitrates were retained until this point, but they were released later as a result of sulphates and arsenic preferential uptake by the resin. BKT curves of sulphates and arsenic in the outlet of column A (Fig. 5) showed similar shape as seen in Fig. 1; however, in the present case, BKT times were much higher due to the significantly lower sulphates concentration in the feed.

By comparing the BKT curves of the different analyzed elements, the following decreasing order of affinity for the strong basic IE resin used in this study could be detected, as also reported by Helferrich (1962): $SO_4^{2-} > HAsO_4^{2-} > NO_3^- > NO_2^- > HCO_3^- > Cl^- > F^- > OH^-$.

BKT curves of column B were very similar to those observed in column A for chlorides, nitrates and bicarbonates. Differently, both sulphates and arsenic con-

centrations in the effluent (Fig. 5) never increased to significant values: for instance, As(V) remained below 10 $\mu\text{g/l}$ for longer than 13,000 V_b treated.

The same configuration plant was also tested with feed F2, spiked with 100 $\text{mg/l } SO_4^{2-}$ and 100 $\mu\text{g/l As (V)}$ (test 28). In this case, three cycles of operation were performed, according to the following layout: (first cycle) A:B, (second cycle) B:A, (third cycle) A:B. Two regeneration steps were also carried out on column A and column B, respectively.

Figures 6 and 7 show the BKT curves of chlorides, nitrates, bicarbonates, sulphates and arsenic at the outlet of column A and B, respectively; the different colors refer to the consecutive cycles of operation.

The behaviour of the different anions with respect to the IE process was very similar to that observed in test 27; however, in this case the higher sulphate content in the feed enhanced the competition of this element versus the others for the IE active sites of the resin. As a consequence, the shape of the BKT curves was steeper and the peaks corresponding to the EX conditions were higher. Furthermore, duration of the operation cycles of the system was shortened as well as the volume of feed water treated per cycle. For

Fig. 5 Breakthrough curves of sulphates and arsenic at outlet of columns A and B in test 27

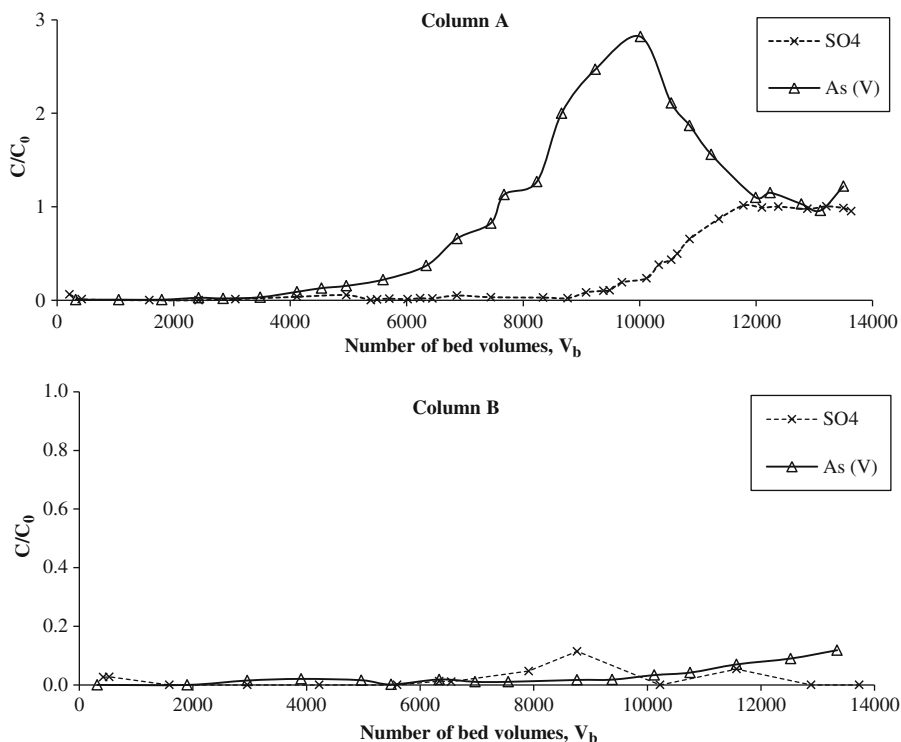


Fig. 6 Breakthrough curves of the main ions at outlet of column A in test 28

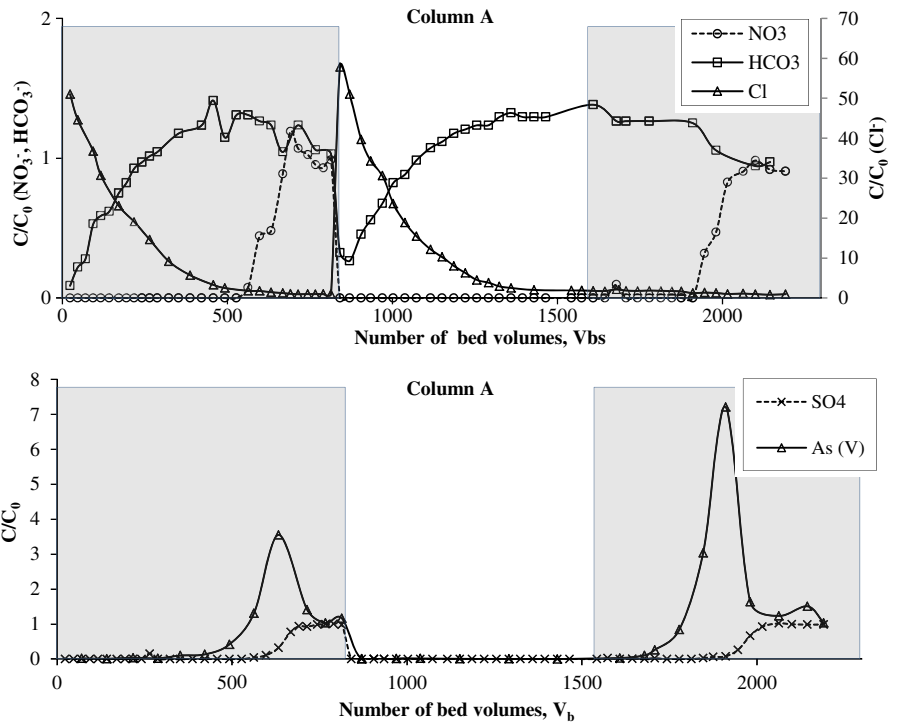
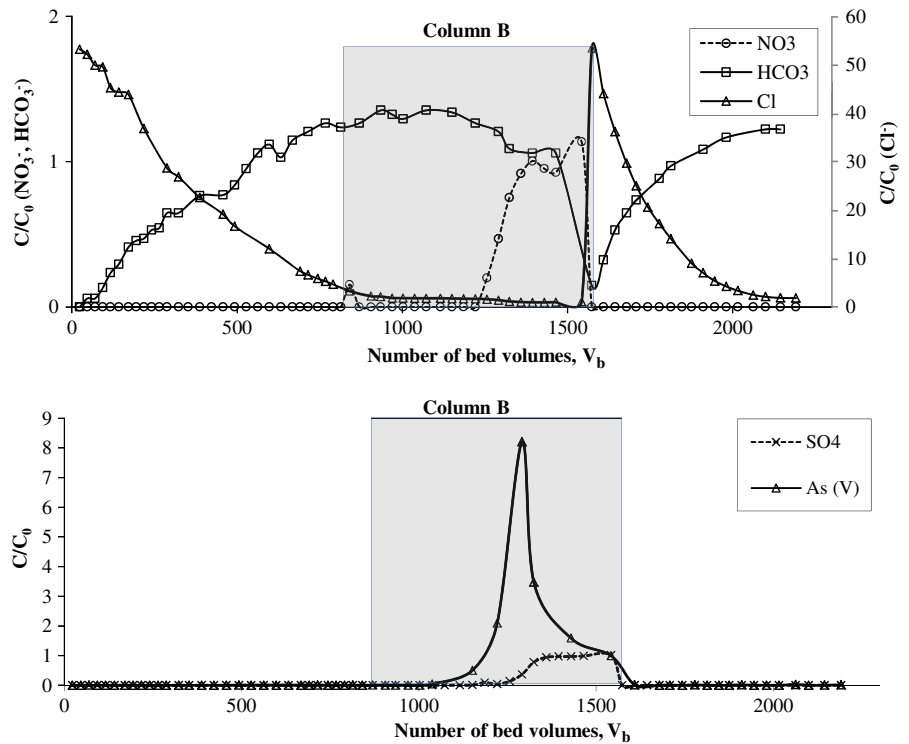


Fig. 7 Breakthrough curves of the main ions at outlet of column B in test 28



instance, in the previously discussed test 27, about 144,500 ml of feed water could be treated per cycle, whereas in this case, a 5-fold sulphate concentration increase determined a significant reduction of the treated volume per cycle to about 11,300 ml.

However, it is worth noting that under these severe conditions, arsenic concentration in the final effluent from the plant was always far below the MAC for drinking water.

Kim et al. (2003) tested the same in series column operation in a laboratory-scale treatment system fed an influent containing a much lower concentration of As(V) (40 µg/l) and also of sulphate (80 mg/l). They achieved an effluent As(V) concentration typically below 1 µg/l; furthermore, a negligible fraction of the sorbed As(V) was released during column regeneration in tests treating more than 36,000 bed volumes of water. In the present study, the same operation strategy demonstrated to be successful also in handling high concentrations of arsenic (100 µg/l) in the presence of relevant contents of sulphates (100 mg/l).

The experimental data from column A were then fitted using the model parameters previously determined. A pretty good agreement between the experimental EX time of sulphates ($t_{EX}=814$) and the value predicted by the model ($t_{EX(M)}=888$ BV) was found.

The efficiency of the regeneration phase, ER%, was then evaluated, making reference to column A between the first and the second cycles of operation, and to column B between the second and the third cycle of operation. The values of ER% were calculated as:

$$ER\% = \frac{SO_4(\text{exp})}{SO_4(\text{theo})} \quad (12)$$

where $SO_4(\text{theo})$ and $SO_4(\text{exp})$ represent the amount of sulphates expected since removed during column service and the content of sulphates measured in the spent brine solution, respectively. For both columns, the obtained regeneration efficiency was very high (approximately 85%). It is worth noting that the spent brine solution contained mainly sulphates, whereas most of the removed arsenic was retained within the column still in operation. Therefore, the brine can be treated through chemical precipitation of sulphates and then be reused in the following regeneration cycles. Details on the treatment and recovery of the spent brine solution according to this procedure can be

found in a previous report of the same authors (Baclocchi and Chiavola 2006).

5 Conclusions

The removal of high concentrations of arsenic from drinking water in the presence of sulphates was studied in laboratory-scale IE packed column experiments. A generic resin without any conditioning was used. The performances of this IE resin were quite satisfactory in terms of the run time observed until the MAC of arsenic was reached in the effluent. The effect of the main operating parameters was evaluated. That is, it was observed that increasing column height, decreasing influent flow rate and decreasing influent contaminant concentrations all resulted in an increase of the breakthrough and exhaustion times. Among these parameters, the system showed to be mainly affected by the change in the contaminant load of the feed water.

The two-in-series column plant, operating by switching the column positions at sulphate exhaustion of the first one, showed to be suitable to treat highly contaminated waters in a full-scale application since it allows to extend service time before arsenic is detected in the final effluent.

The three different models applied to the experimental data of the breakthrough curves described reasonably well the experimental breakthrough data collected in both single column and two-in-series column system. The values of the maximum IE capacity, q , and of the rate constant, k , were determined to be 3.8 mEq/g and 0.57 l/h mEq, respectively. These parameters were successfully used to predict the operation of the column plant under real conditions.

References

- American Public Health Association/American Water Works Association/Water Environment Federation (APHA/AWWA/WEF). (1998). *Standard methods for the examination of water and wastewater* (19th ed.). Washington: American Public Health Association/American Water Works Association/Water Environment Federation.
- Baclocchi, R., & Chiavola, A. (2006). Ion exchange process in the presence of high sulphate concentration: resin regeneration and spent brine reuse. *Water Science and Technology-Water Supply*, 6(3), 35–41.

- Baclocchi, R., Chiavola, A., & Gavasci, R. (2005). Ion exchange equilibria of arsenic in the presence of high sulphate and nitrate concentrations. *Water Science and Technology-Water Supply*, 5(5), 67–74.
- Benfield, L. D., Judkins, J. F., Jr., & Weand, B. L. (1982). *Process chemistry for water and wastewater treatment*. Englewood Cliffs: Prentice-Hall.
- Bohart, G. S., & Adams, E. Q. (1920). Some aspects of the behavior of charcoal with respect to chlorine. *Journal of the American Chemical Society*, 42, 523–544.
- Borba, C. E., da Silva, E. A., Fagundes-Klen, M. R., Kroumov, A. D., & Guirardello, R. (2008). Prediction of the copper (II) ions dynamic removal from a medium by using mathematical models with analytical solution. *Journal of Hazardous Materials*, 152, 366–372.
- Clifford, D. (1999). Ion exchange and inorganic adsorption. In American Water Works Association (Ed.), *Water quality and treatment: a handbook of community water supplies* (5th ed.). New York: McGraw-Hill.
- Clifford, D., & Ghurye, G. (2001). *Laboratory study on the oxidation of arsenic(III) to arsenic(V)*. EPA/600/R-01/021.
- Frankenberger, W. T., Jr. (2001). *Environmental chemistry of arsenic*. New York: Marcel Dekker.
- Ghurye, G. L., Clifford, D. A., & Tripp, A. R. (1999). Combined arsenic and nitrate removal by ion exchange. *Journal of American Water Works Association*, 91(10), 85–96.
- Helfferich, F. (1962). *Ion exchange*. New York: McGraw-Hill.
- Jain, C. K., & Ali, I. (2000). Arsenic: occurrence, toxicity and speciation techniques. *Water Research*, 34(17), 4304–4312.
- Kim, K., & Benjamin, M. M. (2004). Modeling a novel ion exchange for arsenic and nitrate removal. *Water Research*, 38, 2053–2062.
- Kim, J., Benjamin, M. M., Kwan, P., & Chang, J. (2003). A novel ion exchange process for as removal. *Journal of American Water Works Association*, 95(3), 77–85.
- Korngold, E., Belayev, N., & Aronov, L. (2001). Removal of arsenic from drinking water by anion exchangers. *Desalination*, 141, 81–84.
- Ming-Cheng, S. (2005). An overview of arsenic removal by pressure-driven membrane process. *Desalination*, 172, 85–97.
- Mohan, D., & Pittman, C. U., Jr. (2007). Arsenic removal from water/wastewater using adsorbents — a critical review. *Journal of Hazardous Materials*, 142, 1–53.
- Mudhoo, A., Sharma, S. K., Garg, V. K., & Tseng, C. H. (2011). Arsenic: an overview of applications, health, and environmental concerns and removal processes. *Critical Review in Environmental Science and Technology*, 41, 435–519.
- Senthilkumar, R., Vijayaraghavan, K., Jegan, J., & Velan, M. (2010). Batch and column removal of total chromium from aqueous solution using *Sargassum polycystum*. *Environmental Progress and Sustainable Energy*, 29(3), 334–341.
- Smedley, P. L., & Kinniburgh, D. G. (2002). A review of the source, behavior and distribution of arsenic in natural waters. *Applied Geochemistry*, 17, 517–568.
- Thomas, H. C. (1944). Heterogeneous ion exchange in a flowing system. *Journal of the American Chemical Society*, 66, 1664–1666.
- Treybal, R. E. (1981). *Mass-transfer operations* (3rd ed.). New York: McGraw-Hill.
- US EPA (2000). *Technologies and costs for removal of arsenic from drinking water*. EPA 815-R-00-028. Washington.
- US EPA (2003). *Arsenic treatment technology. Evaluation Handbook for Small Systems*. EPA 816-R-03-014. Washington.
- Viraraghavan, T., Subramanian, K. S., & Aruldoss, J. A. (1999). Arsenic in drinking water – problems and solutions. *Water Science and Technology*, 40(2), 69–76.
- Yan, G., Viraraghavan, T., & Chen, M. (2001). A new model for heavy metal removal in a biosorption column. *Adsorption Science and Technology*, 19, 25–43.